THE ASTRONOMICAL JOURNAL VOLUME 73, NUMBER 10, PART 1 DECEMBER 1968

Measurements of the Flux Density and Spectra of Discrete Radio Sources at Centimeter Wavelengths. II. The Observations at 5 GHz (6 cm)

I. I. K. Pauliny-Toth and K. I. Kellermann
*National Radio Astronomy Observatory, Green Bank, West Virginia**
(Received 16 September 1968)

The flux densities of 480 sources have been measured at a frequency of 5.0 GHz (6 cm) using the 140-ft telescope of the National Radio Astronomy Observatory. These include almost all extragalactic sources in the Revised 3C catalogue and a number of other sources, particularly from the various Parkes catalogues. An accuracy of measurement of better than 0.05 flux unit (1 flux unit $= 10^{-26}$ W/m²/Hz) has been achieved for the majority of the sources. A number of interesting optical objects such as Seyfert and compact galaxies and "radio quiet" quasistellar galaxies were also observed and radio emission was detected in some of these. The distributions of spectral indices between 6 and 11 cm for radio galaxies, quasistellar sources, and unidentified sources have been compared with the corresponding distributions between 21 and 11 cm. Two classes of sources can be distinguished: those with a narrow dispersion of spectral indices about a median value near -0.8 and those with a much larger dispersion of indices about a median value near zero. This separation is more pronounced at centimeter than at longer wavelengths. Radio galaxies, quasistellar sources detected by surveys at meter wavelengths, and unidentified sources fall mainly in the first class; sources in the second class are mainly quasistellar sources detected by surveys at decimeter wavelengths. Unidentified sources tend to have steeper spectra than radio galaxies or quasistellar sources. The spectral index of radio galaxies between 21 and 11 cm is the same as between 11 and 6 cm.

I. INTRODUCTION

THE measurements described in the present paper form part of a program aimed at determining the spectra of extragalactic radio sources at centimeter wavelengths. The observations at 2695 MHz (11.3 cm) have already been reported in Paper I (Kellermann, Pauliny-Toth, and Tyler 1968) and those at 15 300 MHz (1.96 cm) will be given in a future paper. The present results and those in Paper I are being used together with other data in an analysis of the spectra of sources in the revised 3C catalogue (Bennett 1962) between 38 and 5000 MHz (Kellermann, Pauliny-Toth, and Williams 1968). The spectra of these and other sources at centimeter wavelengths are discussed further in this paper.

The sources observed include nearly all extragalactic sources in the revised 3C catalogue as well as a number of other sources chosen from the 3C catalogue (Edge, Shakeshaft, McAdam, Baldwin, and Archer 1959), from the CTA (Harris and Roberts 1960) and CTD (Kellermann and Read 1965) lists, from the Parkes surveys (Bolton, Gardner, and Mackey 1964; Day, Shimmins, Ekers, and Cole 1966; Shimmins, Day, Ekers, and Cole 1966) and from the NRAO catalogue (Pauliny-Toth, Wade, and Heeschen 1966). In the selection of sources from lists other than the revised 3C catalogue, preference was given to sources identified with optical objects and to sources which were expected to have relatively high flux densities at 6 cm on the basis of their spectra at longer wavelengths. Thus, for unidentified sources, there is an emphasis on objects with flat spectra and this should be borne in mind in any statistical use of the data for these sources. In addition to these known radio sources, a search was made for radio emission from a number of optically interesting objects such as blue stellar objects (quasistellar galaxies), Seyfert galaxies, and a compact galaxy. These are discussed separately in Sec. VII.

* Operated by Associated Universities, Inc., under contract with the National Science Foundation.

II. THE OBSERVATIONS

The observations were made during several periods, in January and February 1966 (I), in April 1967 (II), in December 1967 (III), and in January 1968 (IV), with the 140-ft telescope of the National Radio Astronomy Observatory. (Some observations were also made in August 1965 with a system of low sensitivity; these have been used only to obtain data for the variable sources.) At 5.0 GHz, the aperture efficiency of the telescope is about 60% at the zenith so that a point source gives an antenna temperature of 0.3°K per flux unit.

During period I, the radiometer consisted of a tunnel diode r.f. amplifier, followed by a detector, an audio amplifier, and a synchronous detector. The total system noise temperature was about 700°K and the bandwidth about 300 MHz with its center frequency at 5.0 GHz. For periods II to IV, a more sensitive system was available, with a cooled parametric amplifier as its first stage. The system noise temperature was 100°K and the bandwidth was 200 MHz.

In all the periods, the input of the receiver was switched electrically between two feed horns, one giving the main beam, directed along the axis of the paraboloid and the other giving a reference beam about 18 min. of arc away. This arrangement reduced the effect of atmospheric fluctuations by about 90% (Baars 1966). The half-power beamwidth was 6.2 min. of arc in the E plane and 5.8 min. of arc in the H plane. The whole feed assembly, including the radiometer, could be rotated about the axis of the paraboloid. The sensitivity of the system in the various periods was such that under good observing conditions the rms

difference between two 30-sec integrations of the output was equivalent to a source in the main beam of about 0.15 f.u. during period I and about 0.03 f.u. during periods II to IV.

In period I, a 10 min on–off observation on a source gave an rms error in the measured flux density of 0.05 f.u. In the other periods, 1 min of observation by the same technique would have given an rms error approaching that due to confusion (0.015 f.u.), and systematic errors, such as those due to incorrect pointing or to partial resolution of the sources, were relatively more important. For this reason, different observing techniques were used during period I and during periods II to IV, as described below.

Period I: Almost all observations during this period were made by the on–off technique and most of the sources observed were known to have an angular size much smaller than the beamwidth. The pointing of the telescope was calibrated beforehand by observing a number of sources of small angular diameter, with accurately known radio or optical positions, over a range of declination from $-35°$ to $+80°$. Some of these sources were also observed over a range of hour angles, in order to determine the change in the pointing corrections with hour angle and also to measure the dependence of the aperture efficiency and of the atmospheric extinction on the orientation of the telescope. The accuracy with which the pointing was known is thought to be better than ± 20 sec of arc in each coordinate, the resulting error in the measured antenna temperature being less than 1%.

Observations were made within one hour of meridian transit, in order to keep the effect of both the change in aperture efficiency with the changing orientation of the telescope and the change in the pointing corrections as small as possible. Each on–off observation consisted of a series of integration periods of 30 sec, taken with the main beam alternately on and off the source, followed by an internal calibration signal from an argon discharge tube. Two such series of on–offs were made for each source: one with the electric vector of the main beam in position angle 0° and the other with the electric vector in position angle 90°. In the first set of on–offs, the reference beam was south of the main beam and the off-source positions were 15 min of arc east and west of the source; in the second set the reference beam was to the west and the off-source positions were 15 min of arc north and south, so that at no time was the source in the reference beam.

The number of pairs of on–off integrations in each series varied from 2 to 5, depending on the expected flux density of the source. On the weaker sources, the resulting rms error in the flux density was about 0.05 f.u. Reference was made to the NRAO list and the Parkes catalogues to ensure that neither the main beam nor the reference beam pointed at other nearby sources. Each series of on–offs was reduced separately and the mean difference between the integrations on and off the source was expressed in terms of the calibration signal. The average of the two series gave a measure of the total flux density, including any linearly polarized component.

For a few sources, which were known to have an angular size comparable with the beamwidth, scans in right ascension and declination were made through the computed position in each of the two orthogonal planes of polarization. The peak of the response, and the broadening of the beam relative to "point" sources at nearby declinations were measured, so that relative flux densities, corrected for the angular size of the source, were obtained in the manner described in the following section.

Periods II to IV: All observations during these periods were made by means of scans in right ascension and declination through the expected position of the source. An angular scan rate of 10 min of arc per minute was used, between limits ± 15 min of arc from the source. Five-second integrations of the output of the receiver were recorded and corresponding integrations of successive scans in the same coordinate were averaged in a computer. Generally, only one or two scans were made in each coordinate, each set being followed by a measurement of the internal calibration signal. The rms error in the measurement of the peak response was typically 0.03 f.u. The scans in right ascension were made with the E vector of the main beam in position angle zero and the declination scans in position angle 90°, the reference beam being south of the main beam in the first case and west of it in the second, so that only the main beam scanned through the source.

In the analysis, a number of points at the beginning and the end of the scan were used to compute a base line, which was then subtracted from the remainder of the scan. Gaussian functions were fitted to the right ascension and declination scans independently and gave in each case a peak, a half-power width, a position for the peak, and the standard error in each of these quantities. If the position derived from the scans differed from the assumed position by more than 30 sec of arc (the corresponding error in the measured peak response being about 1%), the observed peak values were corrected by the appropriate amount. The average of the peaks derived from the right ascension and declination scans was then obtained, giving a measure of the total density for sources small compared with the beamwidth, independent of any linearly polarized component. The product of this average and the computed half-power widths in right ascension and declination was also obtained and gave a measure of the integrated flux density for sources of any angular size, provided that the response remained Gaussian.

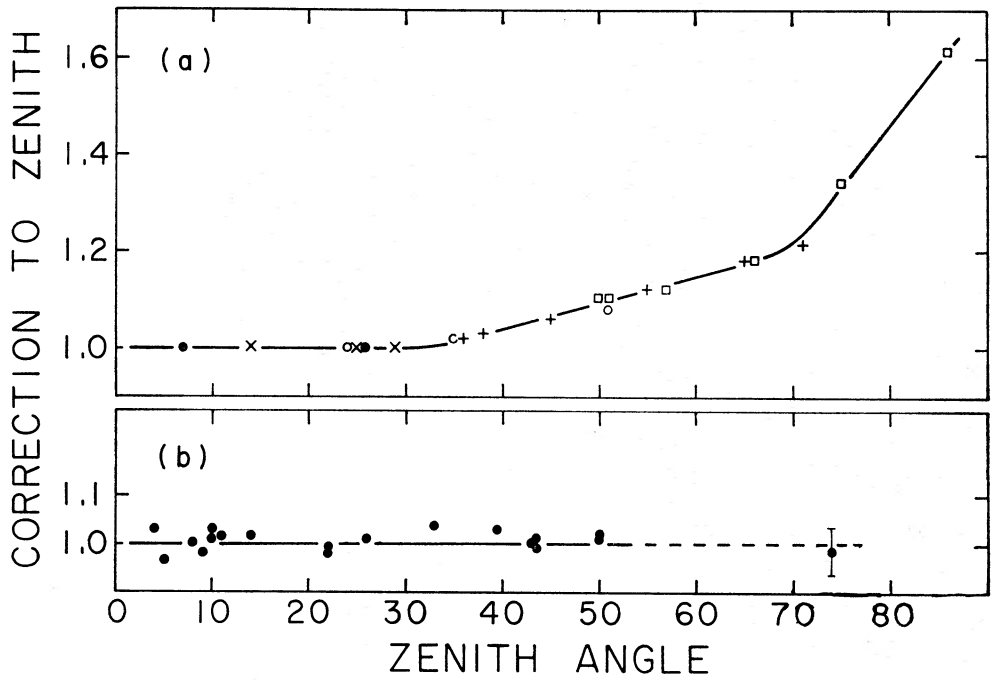

FIG. 1. (a) The factor by which the observed peak antenna temperature of a source of small angular size must be multiplied to obtain the antenna temperature that would be observed at the zenith (period I). The curve was obtained by tracking a number of radio sources of small angular size; these are denoted by the various symbols. (b) A similar correction factor for the "integrated response" (peak multiplied by response widths in R.A. and Dec.), for period III. This curve was obtained from observations of a number of radio sources of small angular size. The relative flux densities of these had previously been obtained using curve a.

III. CALIBRATION OF THE SCALE OF FLUX DENSITY

During Period I, the observations of sources of small angular size over a range of hour angles showed that to within about 3% the gain of the telescope was a function of zenith angle alone down to a zenith angle of 50°. From these observations, a curve was obtained (Fig. 1, curve a) which allowed an observation of a source made at any zenith angle to be corrected to a zenith angle of 0°. This curve included the changes in both the gain of the telescope and in the atmospheric extinction with the zenith angle. All observations of sources of small angular size were reduced to the zenith by means of this curve and thus relative flux densities for these sources were obtained.

The decrease in gain of the telescope with increasing zenith angle is accompanied by an increase in the half-power beamwidth, so that the product of the peak response and the beamwidths in right ascension and declination is less dependent on the zenith angle than the peak response itself. During periods II to IV this "integrated response" was computed for each source as well as the peak response. The relative flux densities of moderately strong sources obtained in period I were then used to calibrate both the peaks and the integrated responses measured in periods II to IV. The calibration curve for the latter (Fig. 1, curve b) was found to have a constant value to within 1% up to a zenith angle of 50°. This confirms the accuracy of the correction curve derived in period I, since any errors in it would be reflected in the curve for the integrated flux densities. Thus, the accuracy in the calibration curves is thought to be about 1% to a zenith angle of 50° ($\delta = -12°$) and is probably better than 5% for the most southerly sources observed ($\delta = -36°$).

The absolute calibration of the flux density scale is described elsewhere (Kellermann, Pauliny-Toth, and Williams 1968). Briefly, it is based on four sources for which flux densities relative to Cas A were available at a number of wavelengths and which were thus found to have power-law spectra to frequencies as high as 8 GHz. These sources were 3C218 (Hydra A), 3C274 (Virgo A), 3C348 (Hercules A), and 3C353. The absolute scale of flux densities is believed to be accurate to 5%.

IV. THE RESULTS

The results are presented in Table I as follows.

Column 1: The most commonly used name of the source. 3C refers to the 3C (Edge *et al.* 1959) or revised 3C (Bennett 1962) catalogues, the latter being distinguished by a digit following the decimal point. P refers to the Parkes catalogues (Bolton *et al.* 1964; Day *et al.* 1966; Shimmins *et al.* 1966) except for P2134+004 (Shimmins, Searle, Andrew, and Brandie 1968). Other symbols used are 4C (Pilkington and Scott, 1965; Gower, Scott, and Wills 1967), NRAO (Pauliny-Toth *et al.* 1966), CTA (Harris and Roberts 1960), CTD (Kellermann and Read 1965), DW (Davis 1967), LHE (Long, Haseler, and Elsmore 1963), and OA (Kraus 1964).

Columns 2 and 3: The flux density and its standard error in flux units. For sources observed by means of scans, the integrated flux density is given if it exceeds the peak flux density by more than the sum of the standard errors. In this case, the peak flux density is given in column 7. Peak flux densities are given where the source is known to be small or where the beam broadening was not significant since the uncertainties

TABLE I. The measured flux densities.

Source	Flux	Err.	Index	Err.	Iden.	Notes	
P0000−17	0.94	0.05	−0.55	0.09	N		
P0003+15	0.40	0.03	−0.33	0.19	QSS		
NRAO 5	1.17	0.05	−0.13	0.09		1	
3C2.0	1.41	0.04	−0.76	0.06	QSS	1	
P0005−06	0.35	0.05	−0.72	0.27			
3C5.	0.50	0.05	−0.97	0.18		1	
3C6.1	1.04	0.04	−0.93	0.07			
3C9.0	0.55	0.05	−0.92	0.17	QSS	1	
P0019−00	1.05	0.04	−0.89	0.08			
3C10.0	21.25	0.38	−0.50	0.04	SNR		(11.52 0.17)
P0023−26	4.13	0.24	−0.50	0.10			
3C11.1	0.82	0.03	−1.13	0.08			
3C13.0	0.40	0.03	−1.32	0.15			
3C14.1	0.67	0.03	−1.01	0.10			
3C14.0	0.61	0.03	−0.80	0.11	GAL		
3C15.0	1.61	0.05	−0.65	0.05	E		
3C16.0	0.51	0.03	−0.99	0.13			
0A33	0.53	0.03	0.21	0.15		2	
3C17.0	2.72	0.07	−0.55	0.05	E		
3C18.0	1.73	0.06	−0.69	0.07	GAL	1	
3C19.0	1.26	0.09	−0.65	0.12		1	
3C20.0	4.18	0.16	−0.70	0.06	GAL		
P0045−25	2.32	0.10	−0.75	0.07	S	1, 3	
3C22.0	0.76	0.03	−0.84	0.09	*GAL		
P0048−09	1.88	0.10	0.78	0.10	GAL	4	(1.75 0.04)
3C26.	0.61	0.04	−1.03	0.13	E	1	
3C27.0	2.48	0.06	−0.88	0.04			
3C28.0	0.45	0.06	−0.65	0.27	GAL		(0.35 0.03)
3C29.0	2.16	0.07	−0.72	0.06	E	1	
3C31.0	2.10	0.07	−0.83	0.13	E		(1.64 0.04)
P0056−00	1.46	0.05	−0.39	0.07	QSS	1	
3C33.2	0.30	0.03	−0.89	0.22			
3C32.	1.08	0.04	−1.07	0.07		1	
3C33.1	0.86	0.03	−1.13	0.08	*GAL		
P0106+01	2.43	0.06	1.28	0.07	QSS	5	(2.30 0.05)
3C33.0	5.03	0.11	−0.57	0.04	E		(4.34 0.07)
3C34.0	0.43	0.03	−0.98	0.15			
3C35.0	0.59	0.06	−1.31	0.18	D		(0.29 0.03)
3C36.0	0.36	0.03	−0.90	0.18		1	
3C38.	1.42	0.07	−1.06	0.08		1	
P0122−00	1.60	0.07	0.17	0.09	QSS		(1.34 0.04)
3C40.0	1.88	0.07	−1.25	0.09	D		(1.14 0.03)
3C41.0	1.46	0.05	−0.68	0.06			
P0124+18	0.61	0.03	−0.60	0.12	E		
3C42.0	0.84	0.04	−1.03	0.09		1	
3C43.0	1.09	0.04	−0.70	0.07	QSS		
P0130−17	0.84	0.04	−0.40	0.09	*QSS		
3C46.0	0.33	0.05	−1.10	0.28	GAL		
3C47.0	1.10	0.05	−1.01	0.08	QSS	1	
3C48.0	5.37	0.07	−0.83	0.03	QSS		
PHL 1093	0.83	0.03	−0.37	0.09	QSS		
3C49.0	0.94	0.06	−0.77	0.12		1	
3C52.0	1.48	0.06	−0.71	0.07	GAL	1	
3C54.0	0.60	0.03	−0.90	0.13			
3C55.0	0.88	0.10	−0.84	0.20	*QSS	6	(0.67 0.04)
4C29.05	0.41	0.03	−0.82	0.08		2	
3C57.	1.25	0.04	−0.74	0.07	QSS	1	
3C58.0	27.24	1.04	−0.19	0.06	*SNR		(21.41 0.80)
NRAO 91	2.27	0.04	−0.45	0.04			
DW0202+31	0.86	0.03	−0.02	0.07		2	
P0202−17	1.60	0.08	0.19	0.09	QSS		(1.46 0.04)
3C59.	0.84	0.03	−0.77	0.08			
3C61.1	1.91	0.06	−1.08	0.05	GAL		(1.74 0.03)
3C62.	1.60	0.08	−0.92	0.09	E	1	
3C63.0	1.09	0.06	−0.84	0.11	E		(0.85 0.03)

TABLE I (*continued*)

Source	Flux	Err.	Index	Err.	Iden.	Notes	
3C66.0	3.75	0.09	−0.84	0.04	E		(2.46 0.05)
3C65.0	0.77	0.05	−1.16	0.13		1	
3C67.0	0.91	0.05	−0.99	0.10	GAL	1	
P0229+13	1.17	0.04	−0.20	0.08	QSS		
3C68.1	0.83	0.03	−0.83	0.08	*GAL		
3C68.2	0.18	0.03	−1.35	0.34			
P0232−04	0.66	0.03	0.03	0.13	QSS		
3C69.0	0.87	0.05	−1.08	0.11		1	
3C71.0	1.90	0.07	−0.74	0.07	SEY		
3C73.	0.67	0.05	−0.82	0.14			
3C75.0	2.36	0.15	−0.71	0.11	DB	6	(1.91 0.07)
3C76.1	1.31	0.04	−0.63	0.06	E		
3C78.0	3.40	0.11	−0.64	0.06	D	1	
3C79.0	1.31	0.04	−1.01	0.06	E	1	
3C83.1	3.53	0.20	−0.52	0.10	E	7	(1.80 0.06)
CTA 21	2.86	0.05	−0.89	0.04			
3C84.0	18.72	0.24	1.03	0.03	SEY	5	
P0320+05	0.88	0.03	−0.77	0.14	GAL		
NRAO 134	0.46	0.03	−0.82	0.09		2	
3C86.0	3.85	0.25	−0.44	0.12			(2.85 0.06)
3C88.0	1.96	0.15	−0.68	0.13	D	6	(1.74 0.07)
3C89.0	0.81	0.06	−0.92	0.14	D		(0.70 0.03)
NRAO 140	2.50	0.06	−0.19	0.05	QSS	5	
3C91.0	1.16	0.04	−0.86	0.07			
CTA 26	2.05	0.05	0.20	0.06	QSS	5	
3C93.0	0.89	0.04	−0.92	0.09	QSS	1	
3C93.1	0.75	0.04	−0.86	0.11	GAL	1	
3C95.	0.73	0.04	−1.10	0.09	QSS		
3C94.	0.70	0.03	−1.13	0.09	QSS		
NRAO 150	7.40	0.13	0.96	0.04		5	
3C98.0	4.97	0.12	−0.56	0.05	E		(4.03 0.08)
3C99.0	0.69	0.03	−0.45	0.11	GAL		
P0359+19	0.38	0.03	−0.45	0.47	E		
P0403−13	2.93	0.09	0.04	0.06	QSS		(2.66 0.05)
3C103.0	1.41	0.04	−0.98	0.06		1, 8	(1.37 0.04)
3C105.0	2.16	0.07	−0.73	0.07		1, 9	(1.96 0.05)
P0405−12	1.85	0.05	−0.39	0.05	QSS		
3C107.0	0.36	0.03	−1.16	0.18			
3C109.0	1.64	0.12	−0.64	0.12	N	1	
P0413−21	1.37	0.11	−0.26	0.13		1	
3C111.0	7.87	0.15	−0.46	0.04			(7.18 0.11)
3C114.0	0.33	0.03	−0.66	0.21	GAL		
P0420−01	3.36	0.09	0.72	0.05	*QSS		(3.12 0.05)
P0422+00	1.21	0.08	0.59	0.13		1	
P0425+17	0.26	0.05	−0.76	0.35		1	
3C119.0	3.42	0.05	−0.73	0.03	QSS	1	
3C120.	5.09	0.08	0.09	0.10	SEY	5	
3C123.0	16.32	0.19	−0.83	0.02	GAL		
3C124.0	0.34	0.03	−0.77	0.20	GAL		
NRAO 190	3.20	0.05	−0.45	0.04			
3C125.0	0.55	0.03	−0.93	0.10			
3C129.0	2.16	0.07	−1.04	0.13	GAL	10	(1.98 0.03)
3C130.0	0.89	0.05	−0.92	0.11	D		(0.78 0.02)
3C131.0	0.86	0.04	−0.89	0.09		1	
3C132.0	1.05	0.04	−1.00	0.08	GAL	1	
P0454+06	0.55	0.05	−0.23	0.18	*QSS	1	
P0458−02	2.18	0.07	0.11	0.06	*QSS		(1.99 0.04)
3C133.0	2.16	0.06	−0.73	0.05		1	
3C134.0	1.95	0.06	−1.26	0.05		1	
3C135.0	1.08	0.06	−0.75	0.11	E		(1.03 0.03)
3C136.1	1.41	0.05	−0.63	0.08	D		(0.94 0.02)
3C137.0	0.57	0.04	−1.00	0.14		1	
3C138.0	4.16	0.07	−0.59	0.03	QSS		
P0521−36	9.33	0.49	−0.31	0.10	N		
3C139.2	0.65	0.05	−0.75	0.15			

TABLE I (*continued*)

Source	Flux	Err.	Index	Err.	Iden.	Notes	
3C141.0	0.55	0.11	−1.14	0.33		1	
3C142.1	1.02	0.04	−0.85	0.07			
3C147.0	8.18	0.11	−0.75	0.03	QSS	1	
3C151.	0.51	0.05	−0.71	0.19		1	
3C152.0	0.25	0.03	−1.93	0.18			
P0604−20	0.86	0.06	−1.22	0.17		1, 9	(0.84 0.06)
P0605−08	3.66	0.06	0.29	0.06		5	
3C153.0	1.35	0.06	−0.87	0.08	GAL	1	
P0607−15	3.13	0.07	0.50	0.05			
3C154.0	2.02	0.05	−0.67	0.05	*QSS	1	
3C158.0	0.63	0.03	−0.93	0.11	*QSS	1	
3C161.	6.73	0.09	−0.80	0.03			
3C165.0	0.77	0.03	−0.88	0.09	*QSS		
3C166.0	1.12	0.03	−0.66	0.06	GAL		
3C169.1	0.40	0.03	−0.40	0.19			
3C171.0	1.22	0.04	−0.80	0.07	GAL	1	
3C173.0	0.52	0.05	−0.81	0.18			
3C172.0	0.85	0.04	−0.94	0.12		1	
3C173.1	0.77	0.06	−1.01	0.14	GAL	1	
3C174.	0.22	0.06	−1.08	0.47		1	
3C175.0	0.66	0.04	−1.02	0.12	QSS	1	
3C175.1	0.56	0.05	−1.09	0.16		1	
3C177.0	0.38	0.04	−1.11	0.20	N		(0.33 0.02)
3C178.	0.33	0.04	−1.29	0.23	S	1	
3C179.	1.31	0.07	−0.29	0.10	S	1	
3C180.0	0.94	0.03	−0.84	0.07	GAL	1	
3C181.0	0.66	0.05	−1.03	0.14	QSS	1	
3C184.0	0.60	0.04	−1.07	0.13		1	
3C184.1	1.24	0.07	−0.73	0.10	D		(1.10 0.04)
P0735+17	1.97	0.14	0.05	0.12		1	
P0736+01	1.65	0.05	−0.34	0.06	QSS	5	
3C186.0	0.38	0.05	−0.67	0.25	QSS	1	
3C187.0	0.39	0.03	−1.05	0.14			
DW0742+10	3.84	0.07	0.03	0.05			
LHE 210	2.85	0.05	−0.85	0.04			
P0745−19	0.46	0.04	−1.08	0.14	D		
3C190.0	0.82	0.06	−0.86	0.14	QSS	1	
3C191.0	0.46	0.06	−1.19	0.23	QSS	1	
3C192.0	2.05	0.06	−0.71	0.05		1, 9	(1.99 0.06)
3C193.	0.43	0.03	−0.86	0.15	E		
P0805−07	1.13	0.04	−0.11	0.15			
3C195.	1.58	0.06	−0.76	0.07	E	1	
3C194.0	0.61	0.03	−0.90	0.11			
3C196.0	4.36	0.06	−0.91	0.03	QSS		
P0812+02	0.78	0.03	−0.61	0.12	QSS	11	
3C196.1	0.47	0.04	−0.79	0.17	D	1	
3C197.1	0.86	0.06	−0.49	0.14	D		(0.66 0.03)
P0818+17	0.61	0.03	−0.88	0.14	GAL		
3C198.0	0.46	0.05	−1.24	0.20	E		(0.42 0.03)
3C200.0	0.66	0.03	−0.84	0.10	GAL		
P0825−20	1.41	0.08	−0.62	0.10	QSS		(1.26 0.04)
4C37.24	0.93	0.03	−0.69	0.03	QSS	2	
3C204.0	0.34	0.03	−0.64	0.18	QSS		
3C205.0	0.67	0.04	−0.82	0.12	*QSS	1	
3C206.	0.63	0.06	−0.87	0.17	QSS	1	
3C207.0	1.44	0.05	−0.34	0.06	QSS	5	
3C208.0	0.54	0.05	−0.91	0.17	QSS	1	
3C208.1	0.71	0.04	−0.88	0.11		1	
3C210.0	0.49	0.08	−1.05	0.31	GAL	1	
3C212.0	0.89	0.04	−0.75	0.09	N	1	
3C213.1	0.84	0.03	−0.30	0.09	GAL		
P0859−25	1.75	0.08	−0.84	0.08			
P0859−14	2.44	0.07	−0.75	0.05	QSS		
4C22.22	0.42	0.08	0.58	0.07	*QSS		(0.24 0.03)
3C215.0	0.41	0.03	−0.85	0.16	QSS		

TABLE I (*continued*)

Source	Flux	Err.	Index	Err.	Iden.	Notes	
3C217.0	0.48	0.06	−1.20	0.22	QSS	1	
3C216.0	1.81	0.04	−0.45	0.05	QSS		
P0906+01	1.12	0.04	−0.12	0.17			
3C218.	13.78	0.17	−0.85	0.03	D		
3C219.0	2.29	0.06	−1.04	0.05	D		
P0922+14	0.31	0.05	−0.40	0.50	QSS		
4C39.25	7.57	0.13	0.83	0.04	QSS		
3C220.1	0.54	0.03	−1.11	0.12	GAL		
3C220.2	0.59	0.03	−0.83	0.11			
3C220.3	0.64	0.05	−1.20	0.18	GAL	1	
3C222.0	0.13	0.03	−1.29	0.39	GAL		
3C223.0	1.29	0.07	−0.75	0.10	E		(0.98 0.03)
3C223.1	0.87	0.05	−0.57	0.11	E	1	
3C225.0	1.26	0.06	−0.92	0.09			(0.90 0.03)
3C226.0	0.64	0.05	−0.99	0.14	GAL		(0.54 0.03)
3C227.0	2.60	0.12	−0.81	0.09		1, 9	(2.40 0.10)
3C228.0	1.14	0.06	−0.89	0.09		1	
3C230.0	0.65	0.03	−1.30	0.10	*QSS	12	
3C231.0	3.94	0.08	−0.56	0.04	I		(3.76 0.05)
3C232.	0.86	0.03	−0.26	0.09	QSS		
P0957+00	0.37	0.04	−0.43	0.23	QSS	1	
3C234.0	1.54	0.05	−1.04	0.06	N	1	
3C236.0	1.34	0.08	−0.66	0.14	D	1, 13	
3C237.0	2.01	0.06	−0.97	0.05	*GAL	1	
3C238.0	0.58	0.04	−1.36	0.13		1	
3C239.0	0.33	0.03	−1.10	0.19			
P1015−31	1.30	0.07	−0.83	0.09			
3C241.0	0.34	0.05	−1.24	0.27		1	
3C244.1	1.12	0.04	−0.89	0.07	GAL	1	
3C245.0	1.39	0.04	−0.66	0.06	QSS	1	
3C246.	0.72	0.04	−0.91	0.11	QSS	1	
4C20.23	0.69	0.03	−0.69	0.05		2	
P1055+01	3.39	0.07	0.13	0.13	QSS	5	(3.20 0.04)
3C247.0	0.95	0.06	−0.92	0.10		1, 9	(0.85 0.06)
3C249.0	0.61	0.09	−1.20	0.25		1	
3C249.1	0.78	0.03	−0.94	0.08	QSS	1	
3C250.0	0.29	0.03	−0.89	0.19			
3C252.0	0.32	0.03	−0.96	0.21			
3C253.	0.45	0.03	−1.06	0.14			
3C254.0	0.79	0.05	−0.98	0.12	QSS	1	
P1115−07	0.26	0.03	−0.76	0.26			
P1116+12	1.64	0.07	−0.16	0.08	QSS		(1.49 0.04)
3C255.0	0.19	0.03	−1.70	0.31	GAL		
3C256.0	0.38	0.05	−0.78	0.25		1	
3C257.0	0.52	0.03	−0.81	0.13			
3C258.0	0.40	0.03	−0.46	0.18	GAL		
P1127−14	7.31	0.15	0.21	0.04	QSS	8	
3C261.	0.34	0.05	−0.99	0.27	QSS	1	
P1136−13	1.90	0.06	−0.59	0.14	QSS		
3C263.0	1.04	0.04	−0.82	0.07	QSS	1	
P1138+01	0.93	0.03	−0.76	0.07			
3C263.1	0.78	0.03	−1.14	0.09	GAL		
3C264.0	2.00	0.07	−0.78	0.07	E	1, 14	
3C265.0	0.63	0.03	−1.30	0.10	*GAL	1	
3C266.0	0.32	0.04	−0.96	0.25	N	1	
3C267.0	0.59	0.07	−1.26	0.20		1	
P1148−00	1.97	0.04	−0.41	0.04	QSS		
4C31.38	0.95	0.03	−0.91	0.09	QSS		
3C268.1	2.62	0.06	−0.69	0.05		1	
3C268.2	0.38	0.03	−1.05	0.17	E		
P1201−041	1.00	0.03	−0.45	0.14	DB		
3C268.3	1.09	0.04	−0.96	0.07		1	
3C268.4	0.60	0.03	−0.91	0.11	QSS		
3C270.0	8.32	0.16	−0.68	0.03	E		(5.46 0.08)
P1217+02	0.56	0.07	0.31	0.25	QSS	1	

TABLE I (*continued*)

Source	Flux	Err.	Index	Err.	Iden.	Notes		
3C270.1	0.87	0.04	−0.88	0.09	QSS	1		
3C272.0	0.36	0.03	−1.07	0.18				
4C21.35	0.76	0.03	−0.44	0.15	QSS			
3C272.1	2.86	0.08	−0.51	0.05	E	1		
3C273.0	43.41	0.50	0.08	0.03	QSS	5		
3C274.0	72.07	1.00	−0.80	0.03	E		(65.75	0.60)
P1229−02	1.32	0.07	−0.05	0.10	QSS		(1.10	0.03)
3C274.1	0.76	0.03	−1.08	0.09	GAL	1, 9	(0.71	0.03)
P1233+16	0.55	0.06	−0.86	0.20	DB		(0.43	0.03)
P1233−24	0.79	0.04	−0.54	0.18	QSS			
P1237−10	1.53	0.05	0.00	0.06	QSS			
3C275.0	0.95	0.05	−1.07	0.10		1		
3C275.1	0.91	0.06	−0.87	0.12	QSS	1		
P1245−19	2.58	0.08	−0.55	0.05				
3C277.0	0.31	0.03	−1.07	0.21				
3C277.1	1.05	0.04	−0.61	0.08	QSS	1		
3C277.2	0.58	0.03	−0.72	0.12				
3C277.3	1.24	0.04	−0.72	0.07	D			
3C278.	2.84	0.07	−0.74	0.05		1, 9	(2.76	0.07)
P1252+11	1.06	0.04	0.11	0.09	QSS	1		
3C279.	15.34	0.27	0.40	0.03	QSS	5		
3C280.0	1.53	0.06	−1.00	0.07		1		
3C280.1	0.36	0.03	−0.87	0.18	QSS			
3C281.	0.31	0.09	−1.13	0.49	QSS	6	(0.24	0.07)
P1306−09	2.00	0.05	−0.62	0.04	D			
3C284.0	0.69	0.06	−0.71	0.16	GAL		(0.58	0.03)
3C283.	1.20	0.05	−1.12	0.08	GAL	1		
3C285.0	0.76	0.05	−0.81	0.13	D	1, 9	(0.73	0.05)
4C22.38	0.33	0.03	0.19	0.28	*QSS			
4C31.42	0.19	0.03	−0.32	0.40				
P1327−21	0.98	0.04	−0.39	0.10	QSS			
3C287.0	3.26	0.06	−0.55	0.04	QSS			
3C286.0	7.48	0.09	−0.51	0.03	QSS			
3C287.1	1.43	0.07	−0.48	0.09	N		(1.26	0.04)
P1335−06	1.06	0.04	−0.81	0.08	QSS			
3C288.0	0.99	0.06	−0.94	0.11	D	1		
3C288.1	0.40	0.03	−1.13	0.16	QSS			
3C289.0	0.60	0.03	−1.07	0.11				
P1345+12	2.71	0.04	−0.51	0.03	S			
3C292.	0.72	0.07	−0.67	0.18		1, 9	(0.67	0.07)
3C293.0	1.87	0.04	−0.71	0.04	D			
P1354+19	1.56	0.05	−0.12	0.06	QSS			
3C294.0	0.28	0.04	−1.08	0.28		1		
3C295.0	6.53	0.08	−0.96	0.03	D			
3C296.0	1.71	0.05	−0.74	0.06	E		(1.40	0.03)
3C297.0	0.64	0.03	−0.73	0.11				
P1416−15	0.85	0.04	−0.58	0.09	*GAL			
3C298.0	1.46	0.05	−1.00	0.06	QSS	1		
P1417−19	0.73	0.04	−0.66	0.10	N			
3C299.0	0.90	0.05	−0.92	0.10	GAL	1		
3C300.0	1.10	0.04	−0.90	0.06	E	1		
4C20.33	0.60	0.03	−0.77	0.11	QSS			
3C300.1	0.94	0.06	−1.07	0.11	*QSS		(0.86	0.03)
P1436−16	0.64	0.04	−0.83	0.11	D			
3C303.0	0.94	0.06	−0.80	0.12		1		
3C303.1	0.46	0.05	−0.46	0.21				
3C305.1	0.46	0.03	−0.84	0.15				
3C305.0	0.92	0.04	−0.93	0.09	S	1		
3C306.	0.71	0.06	−0.65	0.15	E		(0.49	0.03)
3C306.1	0.75	0.06	−0.66	0.15	E		(0.61	0.03)
3C308.	0.54	0.03	−0.77	0.06		1, 2		
P1454−06	0.73	0.03	−0.20	0.11	QSS			
P1453−10	1.57	0.05	−0.71	0.06	QSS			
3C309.	0.14	0.04	−0.70	0.59		1		
3C309.1	3.76	0.06	−0.56	0.04	QSS	1		

TABLE I (*continued*)

Source	Flux	Err.	Index	Err.	Iden.		Notes	
3C310.0	1.28	0.07	−1.47	0.10	DB		(1.05	0.03)
3C311.	0.47	0.04	−0.87	0.17		1		
P1504−167	1.89	0.05	−0.34	0.14	*GAL			
P1505+01	0.28	0.03	−1.25	0.23				
NRAO 468	0.43	0.03	−0.83	0.15				
P1508−05	2.28	0.05	−0.35	0.13				
3C313.0	1.39	0.07	−0.65	0.09	E		(1.13	0.03)
3C314.1	0.33	0.03	−1.22	0.19	D			
P1510−08	4.36	0.08	0.78	0.04	QSS	5		
3C315.0	1.27	0.04	−1.00	0.05	DB	1		
P1514+00	1.54	0.05	−0.27	0.14	QSS			
3C317.0	0.87	0.04	−1.44	0.09	N	1		
P1514−24	2.26	0.10	0.35	0.19	E	5	(2.09	0.04)
3C318.0	0.75	0.03	−0.93	0.09	GAL	1		
3C319.0	0.65	0.03	−1.07	0.10	GAL			
P1523+03	0.68	0.04	−0.69	0.12	E	1		
P1524−13	1.10	0.04	−0.71	0.04	*QSS	2		
3C320.0	0.50	0.03	−0.97	0.13	GAL			
3C321.0	1.22	0.04	−0.83	0.07				
3C322.0	0.46	0.03	−1.01	0.14	GAL			
P1539−09	0.71	0.03	−0.57	0.18				
3C323.0	0.33	0.06	−1.10	0.32	*GAL	1		
3C323.1	0.92	0.07	−0.55	0.14	QSS	1		
3C324.0	0.61	0.03	−1.17	0.10				
DW1548+05	2.54	0.06	0.03	0.07		5		
3C325.0	0.83	0.04	−1.29	0.09		1		
3C326.0	0.48	0.03	−1.63	0.15	GAL			
3C326.1	0.86	0.06	−0.74	0.17			(0.75	0.03)
DW1555+00	1.71	0.05	0.28	0.12		5		
3C327.0	2.76	0.08	−1.03	0.05	D		(2.31	0.03)
3C327.1	1.10	0.04	−1.05	0.07	*GAL	1		
P1602−09	1.17	0.05	−0.81	0.16			(0.99	0.03)
CTD 93	1.67	0.04	−0.88	0.05	GAL			
3C330.0	2.35	0.08	−0.76	0.06			(2.18	0.04)
3C333.	0.73	0.06	−0.47	0.15			(0.57	0.03)
3C332.0	0.83	0.03	−0.93	0.08	D			
3C334.0	0.57	0.03	−1.36	0.11	QSS			
3C336.0	0.69	0.06	−1.14	0.15	QSS	1		
3C341.0	0.57	0.04	−1.15	0.12		1, 15	(0.52	0.03)
3C338.0	0.49	0.03	−1.52	0.10	D			
3C337.0	0.91	0.03	−0.88	0.12				
3C340.0	0.69	0.03	−1.09	0.09				
3C343.0	1.49	0.04	−0.94	0.05				
3C343.1	1.20	0.04	−1.01	0.06				
NRAO 512	1.41	0.04	0.57	0.08	QSS		(1.32	0.02)
3C345.0	5.65	0.08	−0.10	0.03	QSS	5		
3C346.0	1.63	0.10	−0.58	0.11	E	6	(1.44	0.06)
3C347.	0.70	0.04	0.05	0.14				
P1644−10	0.94	0.04	−0.66	0.19				
P1645+17	1.20	0.05	−0.10	0.09				
3C348.0	11.89	0.22	−1.02	0.03	D		(11.10	0.10)
P1648−06	0.82	0.03	−0.64	0.17				
3C349.0	1.14	0.04	−0.80	0.07	GAL			
3C351.0	1.21	0.05	−0.84	0.08	QSS	1		
3C352.0	0.47	0.03	−1.15	0.14				
P1712−03	0.74	0.06	0.25	0.17			(0.51	0.03)
3C353.0	21.49	0.29	−0.78	0.03	D		(18.72	0.15)
3C356.0	0.71	0.03	−0.06	0.17				
3C357.0	1.00	0.13	−0.96	0.07	E		(0.42	0.03)
3C358.	7.29	0.22	−0.53	0.05	SNR		(6.77	0.10)
NRAO 530	4.85	0.08	0.09	0.04		5		
P1732−09	1.04	0.05	−0.55	0.09				
3C368.0	0.21	0.03	−1.16	0.30				
4C27.41	0.90	0.03	0.28	0.11				
3C371.0	1.74	0.05	−0.16	0.05	N	5		

TABLE I (*continued*)

Source	Flux	Err.	Index	Err.	Iden.	Notes		
3C379.1	0.66	0.05	−0.84	0.14		1		
3C380.0	7.50	0.09	−0.45	0.03	QSS	5		
3C381.0	1.29	0.05	−0.94	0.07	E	1		
3C382.0	2.22	0.07	−0.74	0.05	D	1, 9	(2.18	0.07)
3C386.0	2.58	0.08	−0.84	0.06	D		(2.35	0.05)
3C388.0	1.77	0.04	−0.91	0.04	D	1		
3C390.0	1.77	0.05	−0.67	0.06				
3C390.3	4.48	0.08	−0.62	0.04	N		(4.04	0.04)
3C391.0	10.07	0.71	−0.37	0.11			(7.95	0.40)
3C394.0	0.96	0.06	−0.72	0.11			(0.79	0.03)
3C395.	1.81	0.15	−0.57	0.14		1		
3C396.0	10.05	0.19	−0.16	0.02			(6.25	0.09)
3C399.1	1.01	0.04	−0.82	0.08				
3C400.1	0.93	0.06	−0.66	0.12			(0.70	0.03)
P1923−18	0.86	0.06	0.41	0.16			(0.64	0.03)
P1930−08	0.94	0.06	−0.11	0.13			(0.66	0.03)
P1938−15	2.31	0.06	−0.87	0.05				
3C401.0	1.37	0.05	−1.14	0.09	GAL	1		
3C402.0	0.92	0.08	−1.04	0.18	*GAL	1, 9	(0.79	0.06)
3C403.0	2.07	0.06	−0.90	0.05	S	1, 9	(2.01	0.06)
3C403.1	0.45	0.06	−1.24	0.24	E		(0.36	0.03)
3C407.	0.54	0.03	−0.26	0.14				
3C408.	0.29	0.03	−1.13	0.22				
3C409.0	3.12	0.05	−1.18	0.03				
3C410.0	3.79	0.06	−0.74	0.03				
3C411.0	0.87	0.06	−1.07	0.12		1		
P2025−15	0.58	0.06	−0.36	0.20			(0.46	0.03)
3C413.	0.43	0.03	−0.88	0.15				
3C415.2	0.32	0.06	−0.90	0.34			(0.22	0.03)
3C418.0	3.79	0.06	−0.35	0.11		5		
3C424.0	0.65	0.03	−1.03	0.08	E			
P2048−14	0.90	0.07	−0.32	0.14	D		(0.76	0.03)
P2053−20	1.09	0.04	−0.53	0.17	E			
P2058−28	2.06	0.09	−0.71	0.07	E			
P2104−25	4.37	0.18	−0.62	0.07	E		(3.60	0.07)
3C427.1	0.96	0.06	−1.15	0.10		1, 9	(0.89	0.05)
NGC 7027	5.75	0.08	0.83	0.03	PLN			
3C428.0	0.43	0.03	−1.99	0.13		16		
3C430.0	3.22	0.09	−0.56	0.05	E		(2.99	0.05)
3C431.0	0.86	0.06	−1.09	0.13			(0.60	0.03)
3C432.0	0.31	0.06	−1.46	0.34	QSS	1		
3C434.0	0.39	0.03	−1.05	0.16				
3C433.0	3.74	0.07	−0.89	0.04	D			
3C435.0	0.56	0.03	−1.03	0.12				
P2127+04	1.93	0.08	−0.70	0.08		1		
P2128−12	2.15	0.05	0.17	0.05	QSS			
3C435.1	0.70	0.03	−0.73	0.06	*QSS	2, 17		
P2134+004	12.02	0.21	0.73	0.05	QSS			
P2135−14	1.31	0.05	−0.74	0.07	QSS			
3C436.0	0.99	0.03	−0.99	0.07	GAL			
3C437.0	0.88	0.06	−0.88	0.12	*QSS	1		
P2145+06	4.71	0.07	0.50	0.06	QSS			
P2146−13	0.67	0.03	−0.62	0.11	QSS			
P2149+17	0.90	0.04	0.26	0.12				
3C438.0	1.54	0.06	−1.20	0.07	*QSS			
P2203−18	4.62	0.12	−0.17	0.05	QSS			
3C440.	1.07	0.07	−0.75	0.12		1		
3C441.0	0.92	0.03	−0.80	0.07	*GAL			
3C444.	2.29	0.06	−1.09	0.05	D		(2.25	0.03)
3C442.0	0.82	0.06	−1.12	0.16	N		(0.58	0.03)
P2216−03	1.47	0.05	0.63	0.08	QSS			
3C445.0	2.04	0.07	−0.74	0.08	N		(1.25	0.04)
PHL 5200	0.06	0.02	−1.19	0.10	QSS	18		
3C446.	4.07	0.08	−0.08	0.04	QSS	5		
3C449.0	1.39	0.07	−0.94	0.09	D		(0.98	0.04)

TABLE I (*continued*)

Source	Flux	Err.	Index	Err.	Iden.	Notes
CTA 102	3.63	0.06	−0.50	0.03	QSS	
3C452.0	3.26	0.10	−0.95	0.05	E	(2.84 0.06)
P2247+14	1.03	0.06	−0.63	0.11		1
3C454.1	0.22	0.06	−1.73	0.46		(0.15 0.03)
3C454.0	0.79	0.03	−0.68	0.09	QSS	
3C454.2	0.76	0.03	−0.85	0.09		
3C454.3	19.71	0.34	0.99	0.03	QSS	5
P2251+11	0.61	0.03	−0.63	0.20	QSS	
3C455.0	0.93	0.10	−0.75	0.18	E	6 (0.84 0.06)
P2300−18	0.82	0.04	−0.17	0.19	N	
3C457.	0.55	0.06	−0.93	0.20		1, 9 (0.53 0.06)
3C456.0	0.67	0.03	−1.12	0.10	E	
3C458.0	0.93	0.06	−0.94	0.12	GAL	(0.84 0.02)
3C459.0	1.36	0.04	−0.84	0.05	N	
3C460.0	0.34	0.03	−1.32	0.18	GAL	
3C462.	1.12	0.10	−0.48	0.15		6 (1.03 0.04)
CTD 141	0.53	0.03	−0.49	0.14	QSS	
P2328+10	0.90	0.03	−0.19	0.09	*QSS	
3C465.0	2.80	0.08	−0.66	0.06	D	(2.14 0.04)
NRAO 718	0.82	0.03	0.19	0.21		
P2345−16	4.13	0.09	1.41	0.05	QSS	5
3C468.1	0.87	0.03	−1.29	0.07		
3C469.1	0.41	0.03	−1.13	0.15		
P2354−11	1.42	0.05	−0.38	0.06	*QSS	
3C470.0	0.55	0.03	−1.03	0.12	GAL	

Notes to Table I

1 Source observed by means of on–offs.
2 No flux density measurement at 11 cm. Spectral index from 21 cm to 6 cm.
3 The structure given by Fomalont (1968) leads to corrections to the peak flux densities of 46% at 6 cm and 13% at 11 cm; the resulting spectral index is −0.34. Not included in spectral statistics, owing to the uncertain corrections.
4 A source with a flux density of 0.54±0.05 f. u. lies 7′.5 east.
5 The 6-cm flux density shows significant variations; it is given at the epoch 1967.3.
6 Source observed by means of on–offs; the correction for beam broadening has been obtained from 21-cm measurements with a 10′.0 beam (Pauliny-Toth, Wade, and Heeschen 1966).
7 Complex source, mapped by scans in right ascension at several declinations. Flux density is twice that measured with the electric vector in P.A. 0°.
8 Correction to peak flux density from structure given by McDonald, Kenderdine, and Neville (1968).
9 Correction to peak flux density from structure given by Fomalont (1968).
10 A "wing" extends about 15′ west of the source and contributes 0.1±0.05 f. u. to the integrated flux density. 3C129.1, lying 12′ east (MacDonald, Neville, and Ryle 1966) was not detected (<0.1 f. u.).
11 A source with a flux density of 0.22±0.05 f. u. lies 9′ east.
12 The flux density and spectral index refer to NRAO 339. NRAO 340 is 11′ east and has a flux density of 0.13±0.05 f. u.
13 According to Fomalont (1968), 25% of the flux density at 21 cm is in a 9′ halo. However, no beam broadening is seen at 11 cm (Paper I) so that the halo may have a steep spectrum. The flux density and spectral index therefore refer to a small component in 3C236.
14 Fomalont (1968) gives a 4′ halo, in disagreement with MacDonald *et al.* (1968). No corrections have been applied.
15 Fomalont (1968) gives a weak source, having about 9% of the flux density of 3C341, 7′ away. The 6-cm measurements (which did not include that source) and the 11-cm flux density (given in Paper I) have been increased accordingly to determine the spectral index of the entire source.
16 A source lies 10′ south, with a flux density of 0.11±0.05 f. u.
17 The flux density and spectral index refer to NRAO 663 only. NRAO 664, however, forms part of the original 3C435.1.
18 Spectral index from 6-cm and 1.7-m (178-MHz) flux densities.

in the peak flux densities are smaller than in the integrated values. In a few cases, where a source having an angular size comparable with the beamwidth was observed by means of on–offs, a correction for the angular size was applied, if it exceeded about 1%. The origin of the correction is then given in the notes following the table and the uncorrected flux density is given in column 7.

Columns 4 and 5: The spectral index between 11 and 6 cm, derived from the present data and the 11-cm flux densities given in Paper I.

Column 6: The optical identification where it is known, with supernova remnants (SNR), H II regions (H II), quasistellar sources (QSS), Seyfert galaxies (SEY), or the various galaxy types defined by Matthews, Morgan, and Schmidt (1964). These are elliptical galaxies (E), D galaxies (D), N galaxies (N), spiral galaxies (S), irregular galaxies (I) and dumb-bell galaxies (db). (G) is used where the galaxy type is unclassified. An asterisk denotes an uncertain identification.

Column 7: The references to footnotes following the table. Peak flux densities are given here for extended sources.

V. SOURCES OF ERROR

These are:

(i) Random errors caused by noise in the receiver and by fluctuations in the emission of the atmosphere or in the gain of the receiver. During the analysis of the data, the standard error in the peak response, and in the case of the scans, in the integrated response as well, was computed for each observation. The error included the effect of the receiver noise and of short-term

atmospheric fluctuations. It was typically 0.05 f.u. for the on–off observations in period I, 0.03 f.u. for peak flux densities, and 0.05 f.u. for integrated flux densities obtained from scans in periods II to IV.

A comparison of the data on sources which were observed two or more times during a given period showed that the standard error of a single observation could be expressed by the relation

$$\text{S.E.} = [\sigma_n^2 + (\sigma_g S)^2]^{\frac{1}{2}} \text{ f.u.}, \quad (1)$$

where S is the flux density of the source. In period I, σ_n was 0.047 and σ_g was 0.016; in the other periods, σ_n was 0.03 for peak flux densities and 0.06 for integrated flux densities, and σ_g varied from 0.014 to 0.020 for both integrated and peak flux densities. The first term in the expression is due to the receiver noise and short-term atmospheric fluctuations and agrees well with the errors derived from the individual observations. The term which depends on flux density can be considered to consist of two parts: that due to the uncertainty with which the amplitude of the calibration signal was determined in about 1 min of integration (about 0.8% in period I and 0.2% in the other periods); and that due to all other effects, such as daily variations in the atmospheric extinction, in the output of the argon discharge tube, gain changes in the antenna or the receiver, or, in the case of on–off observations, changes in the pointing of the telescope (all these contributing between 0.013 and 0.020 to σ_g). The first term dominates for weak sources, while the second is important for sources stronger than 2 to 3 f.u.

(ii) Errors resulting from confusion by unresolved sources in the main beam or in the reference beam. The results of a 6-cm survey of a small region of sky (Kellermann, Pauliny-Toth, and Davis 1968) show that the rms level of confusion with this system σ_c is about 0.015 f.u.

(iii) Errors in the calibration of the pointing for the on–off observations. The pointing was believed to be known to ±20 sec of arc, a value which gives an error of less than 1% in the measured flux densities. Day-to-day changes in the pointing with an rms amplitude of 15 sec of arc were known to occur. The effect of these is to contribute about 0.005 to σ_g in Eq. (1).

(iv) Errors in the assumed positions of the sources. These also only affect the on–off measurements. The only positions which may have introduced significant errors are those from the Parkes catalogue (up to 1 min of arc, corresponding to an error of 6%) and from the NRAO catalogue (about 30 sec of arc, corresponding to an error of 1.5%).

(v) The uncertainty in the calibration curves which were used to correct for changes in the gain of the telescope and in the atmospheric extinction with zenith angle. Such an uncertainty affects the relative flux densities of sources at different declinations. As was described above, the uncertainty at zenith angles smaller than 50° (declination north of −12°), where no correction for the integrated response is required, is believed to be less than ±1%. For the most southerly sources observed (Parkes 0521–36), the uncertainty may be as high as ±5%.

(vi) The uncertainty in the absolute scale of flux densities. This depends on the uncertainty in the absolute spectrum of Cas A and in the ratios of the 4 standard sources to Cas A. The error due to the latter effect can be estimated from the scatter of the calibration factor for the present observations, derived from each of these sources. The standard error in this calibration factor is 1%. The main uncertainty is therefore that in the absolute measurements of Cas A, that is, about 5%.

(vii) Systematic errors caused by partial resolution of sources. Most of the sources not known to be small compared with the beamwidth were observed by scans. In the case of on–off observations, corrections based on the source structure have been applied in the few cases where they were necessary.

For sources observed by means of scans, integrated flux densities have been given only when they exceed the peak flux densities significantly. To check whether this procedure leads to a systematic error for sources which are barely resolved, we have computed the ratio R of the integrated to the peak flux density from the scans for the three groups of sources discussed in Sec. VIII: radio galaxies, quasistellar sources, and unidentified 3C sources at high galactic latitudes. The mean value of R was

$$\begin{aligned} \text{for radio galaxies: } & \bar{R} = 1.122 \pm 0.018, \\ \text{quasistellar sources: } & \bar{R} = 1.005 \pm 0.010, \\ \text{unidentified 3C sources: } & \bar{R} = 1.014 \pm 0.031. \end{aligned}$$

These mean values of R are within 1% of those obtained from the flux densities in Table I for the same groups of sources and we conclude that no significant systematic error due to partial resolution is present in these data.

It is important to note that any observations which do not take into account the systematic difference between the angular sizes of radio galaxies and quasistellar sources *will* lead to systematic errors in the comparison of their spectra.

The errors quoted in Table I are given by the expression

$$\text{S.E.} = \left(\frac{\sigma_n^2 + \sigma_g^2 S^2}{n} + (\sigma_z^2 + \sigma_p^2) S^2 + \sigma_c^2 \right)^{\frac{1}{2}} \text{ f.u.}, \quad (2)$$

where n is the number of observations, σ_n and σ_g are the noise and gain errors defined in (1), σ_z is the uncertainty in the zenith angle correction and varies from 0.01 north of Dec. −12° to 0.05 at Dec. −36°, σ_p applies only to on–off observations and is the error due

TABLE IIa. Flux densities of sources which were observed repeatedly at 6 cm. This table shows sources which showed significant variations. Flux densities at epoch 1965.0 are from Kellermann (1966).

Source \ Epoch	1965.0	1965.6	1966.1	1967.3	1967.9	1968.1	Notes
P0106+01			1.51±0.05	2.43±0.04	3.82±0.06		1
3C84		15.2±0.4	15.93 0.15	18.72 0.15	19.83 0.25	20.87±0.30	
NRAO 140			2.12 0.08	2.50 0.05	2.49 0.06		
CTA 26	2.8±0.3		1.88 0.06	2.05 0.04	2.10 0.04		
NRAO 150		6.6 0.4	5.56 0.12	7.40 0.11	7.06 0.10		
3C120	3.9 0.5	4.1 0.3	3.33 0.05	5.09 0.06	8.55 0.12	9.62 0.08	
P0605−08				3.66 0.04	3.94 0.08		
P0736+01	1.7 0.3		1.52 0.10	1.65 0.04	1.73 0.04		
3C207			1.53 0.05	1.44 0.04	1.40 0.04		
P1055+01			4.00 0.30	3.39 0.06	3.57 0.09	3.57 0.08	1
P1127−14				7.31 0.11	7.53 0.07		
3C273	40.4 4.0	38.6 0.6	37.60 0.25	43.41 0.25	38.00 0.71	37.80 0.40	
3C279	15.4 1.5	13.8 0.4	12.66 0.10	15.34 0.22	15.94 0.30	16.22 0.16	
P1510−08			2.76 0.08	4.36 0.07	4.50 0.08	3.53 0.04	
P1514−24			2.73 0.12	2.26 0.07			
DW 1548+05				2.54 0.05		2.77 0.05	
DW 1555+00				1.71 0.04		1.93 0.04	
3C345		6.2 0.2	5.62 0.06	5.65 0.06	6.46 0.13	6.86 0.09	
NRAO 530		4.8 0.2	4.16 0.11	4.85 0.05	4.18 0.08	4.54 0.06	
3C371			1.81 0.04	1.74 0.04	1.68 0.04		
3C380			7.18 0.10	7.50 0.05	7.57 0.15		
3C418			3.91 0.10	3.79 0.04	3.78 0.08	3.64 0.06	
3C446			3.92 0.10	4.07 0.07	4.42 0.09	4.42 0.06	
3C454.3	13.3 1.3	10.9 0.4	11.93 0.10	19.71 0.28	22.40 0.30	21.90 0.15	
P2345−16				4.13 0.05	3.56 0.07		

TABLE IIb. Flux densities of sources which were observed repeatedly at 6 cm. This table shows sources which did not vary significantly. Flux densities at epoch 1965.0 are from Kellermann (1966).

Source \ Epoch	1965.0	1965.6	1966.1	1967.3	1967.9	1968.1	Notes
3C48		5.3±0.2	5.25±0.19	5.40±0.08	5.44±0.11	5.38±0.08	
NRAO 91			2.26 0.07	2.29 0.04	2.24 0.05		
3C71	2.0±0.3		1.91 0.05		1.88 0.08		
NRAO 190			3.20 0.20	3.18 0.04	3.21 0.07		
3C138	4.1 0.5		4.15 0.06		4.15 0.08		
3C161	7.2 0.8	6.8 0.3	6.70 0.08	6.69 0.10	6.81 0.13		
3C196			4.44 0.04	4.33 0.05	4.30 0.09	4.35 0.07	
4C39.25				7.49 0.15	7.56 0.11	7.64 0.08	
3C286		7.3 0.3	7.57 0.07	7.45 0.08	7.37 0.14	7.48 0.11	
3C295		6.9 0.4	6.53 0.04	6.65 0.10	6.39 0.12	6.53 0.06	
P2145+06	5.1 0.6		4.57 0.20	4.70 0.07	4.72 0.09		
CTA 102	4.3 0.5	4.2 0.4	3.70 0.08	3.59 0.07	3.58 0.05		2

1 Integrated flux density.
2 Possible slow decrease in flux density.

to the uncertainty in the assumed source position, and σ_c is the rms confusion error (0.015 f.u.). In cases where the quality of individual observations was noticeably poor, the errors have been increased accordingly.

VI. VARIABLE SOURCES

A number of sources, including known or suspected variables and some other moderately strong sources, were observed in two or more periods. The flux densities are given in Table II, together with those measured in August 1965 and those obtained at Parkes (Kellermann 1966). The data on variable sources which we have previously published (e.g., Pauliny-Toth and Kellermann 1966; Kellermann and Pauliny-Toth 1968a and 1968b; Pauliny-Toth and Kellermann 1968) were based on a preliminary scale of flux density, in which the flux density of 3C218 at 6 cm is 13.0 f.u. The present flux densities are based on four standard sources as described in Sec. III, and are 6% higher than the previously published values. The errors in Table II do not include confusion or uncertainties in the correction for zenith angle, since these remain constant for a given source.

The observed time variations at 5.0 GHz are in full agreement with a previous suggestion that flux density increases occur only at wavelengths where the source, or at least one of its components, is optically thick and decreases where it is optically thin as is predicted by an expanding source model. Medd, Locke, Andrew, and van den Bergh (1968) have found variations over a period of $1\frac{1}{2}$ yr at 10 GHz in 3C48, 3C138, 3C196, and 3C286, all of which have "normal" power-law spectra at centimeter wavelengths and also in NRAO 140 and

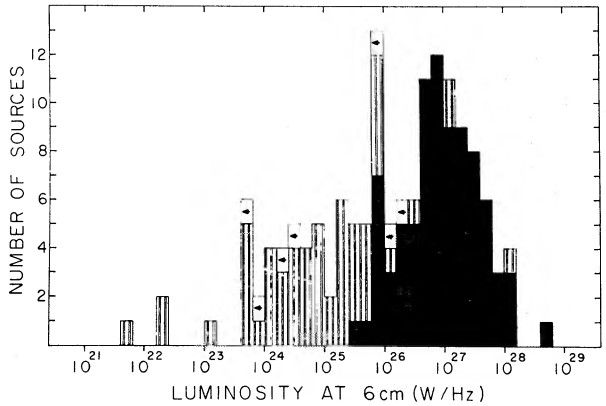

FIG. 2. Histogram of the distribution of the 6-cm luminosity for quasistellar sources (blackened), radio galaxies (vertical hatching) and the upper limits on the 6-cm luminosity of seven blue stellar objects (shown as arrows).

CTA 102, which they describe as having "curved" spectra. At 5 GHz, we find no variations in 3C48, 138, 196, and 286 greater than 2–3% over 2 yr. CTA 102 may possibly be slowly decreasing in flux density but the results are barely significant. NRAO 140 does vary at 6 cm, but its spectrum near this wavelength is complex (Kellermann and Pauliny-Toth 1968c), indicating the presence of several optically thick components. It is of course possible that weak outbursts may occur in a source having a spectrum which is approximately a power law and may cause minor fluctuations in the intensity and spectrum. This, however, does not invalidate the model of an expanding source unless it is determined that the spectrum follows a power law to an accuracy comparable with the observed fluctuations.

VII. BLUE STELLAR OBJECTS AND SEYFERT GALAXIES

In addition to known radio sources, a number of interesting optical objects, previously classified as "radio-quiet," were observed. These include Seyfert galaxies, a compact galaxy and several blue stellar objects, which all have optical properties similar to those of strong radio sources. The results of observations made in period I have already been reported (Kellermann and Pauliny-Toth 1966). In periods III and IV, a number of additional blue stellar objects, taken from the list of Sandage and Luyten (1967), were observed and some of the Seyfert galaxies were reobserved to improve the experimental accuracy. These later observations were made in one plane of polarization only, by pointing the main beam and reference beam alternately towards the optical position, so that the sensitivity was twice that of simple on–off observations using the main beam alone. The results are given in Table III; the quoted errors in the flux density include the random noise and the confusion error of 0.015 f.u. Redshifts and radio luminosities at 6 cm, or upper limits corresponding to twice the standard error are given where appropriate [the luminosity was taken to be proportional to (flux density) $\times$ (redshift)^2].

TABLE III. Measurements of blue stellar objects and Seyfert galaxies. The flux density at 6 cm and its standard error, the redshift, and 6-cm luminosity are given.

Object	Flux density (f.u.)		Redshift	6-cm luminosity (W/Hz)
Blue stellar objects				
PHL 1027	−0.004	±0.018		
PHL 1070	0.002	0.019		
PHL 1072	0.025	0.025		
PHL 1092	−0.004	0.016		
PHL 1106	−0.005	0.018		
PHL 1127	0.008	0.020	1.990	$<2.0\times10^{26}$
PHL 1186	0.005	0.020		
PHL 1194	0.008	0.020	0.298	$<5.0\times10^{24}$
PHL 1222	0.027	0.020		
PHL 1226	0.004	0.019		
PHL 3424	−0.002	0.018	1.827	$<1.3\times10^{26}$
PHL 3375	0.000	0.025		
BSO 1	−0.013	0.028	1.241	$<7.0\times10^{25}$
TON 256	0.000	0.023	0.1307	$<8.5\times10^{23}$
TON 730	−0.002	0.027	0.0877	$<4.3\times10^{23}$
BSO 2	0.008	0.041	0.186	$<3.4\times10^{24}$
BSO 11	−0.115	0.040	2.084	*
Seyfert galaxies				
NGC 3227	0.038	0.018	0.00335	4.6×10^{20}
NGC 3516	0.034	0.025	0.00926	3.1×10^{21}
NGC 4051	0.056	0.030	0.00233	3.3×10^{20}
NGC 4151	0.152	0.018	0.00330	1.8×10^{21}
NGC 5548	0.038	0.021	0.0166	1.1×10^{22}
Compact galaxy				
I ZW 1727+50	0.20	0.03	<0.07	$<7.8\times10^{23}$

* Grossly confused.

Investigation of possible radio emission from these objects is important to clarify their relationship, if any, with similar objects which are strong radio sources. Although all five of the Seyfert galaxies were detected, their 6-cm luminosities, which range from 3×10^{20} to 10^{22} W/Hz, are not significantly greater than those expected from a random sample of normal spiral galaxies, and are 4 orders of magnitude lower than the luminosity of a typical radio galaxy. One galaxy, NGC 4151, was previously known to be a radio source (Heeschen and Wade 1964; De Jong 1967) and its radio spectrum appears to be of the normal power-law type. The data for the other Seyfert galaxies at other frequencies are not accurate enough to allow the spectrum to be determined.

Also detected was the compact galaxy I Zwicky 1727+50 (Zwicky 1966), which was described as a radio-quiet, optically variable object similar in its optical properties to the variable radio source, 3C120, by Oke, Sargent, Neugebauer, and Becklin (1967). The redshift of the source is not known, but is estimated by Oke *et al.* to be less than 0.07, so that the 6-cm luminosity of this source is less than 10^{24} W/Hz, almost a factor of 10 lower than that of 3C120 at its minimum luminosity. We have measured the flux density of 1727+50 at 2.7 GHz to be 0.25±0.10 f.u.

Thus, as in 3C120, the spectrum at centimeter wavelengths is flat, as is characteristic of sources composed of several optically thick components.

For only two blue stellar objects, PHL 1072 and PHL 1222, is there evidence of significant radio emission. The latter has also been observed by us at 15 GHz (0.057±0.015 f.u.) and by Braccesi (1967) at 2.8 GHz (0.10±0.03 f.u.). It too has a spectral index near zero. Kuril'chik and Kokin (1967) have measured flux densities of 0.8 and 0.6 f.u., respectively, for BSO 1 and TON 730 at 3.7 GHz in June 1966. We find no emission from either object at 5 GHz in February 1966 or at 2.7 GHz in April 1967. (The upper limits at 2.7 GHz are 0.08 f.u.) Since these upper limits are an order of magnitude lower than the flux densities reported by Kuril'chik and Kokin, we have strong reservations about their results.

We summarize our observations of blue stellar objects, Seyfert galaxies, and compact galaxies in relation to identified radio sources in Fig. 2, which shows the distribution of the 6-cm luminosity for quasistellar sources (QSS) and radio galaxies. As is well known, the luminosity distribution of radio galaxies and QSS covers a range of more than six orders of magnitude, with QSS dominating the high-luminosity end. None of the BSO's for which redshifts were available were detected; the upper limits on their 6-cm luminosity, which are shown as arrows in Fig. 2, are two or three orders of magnitude less than the luminosities of most quasistellar sources, but not much less than those of the weakest quasistellar sources. These upper limits on the radio luminosity of the "radio-quiet" blue stellar objects lie in the same range as the radio galaxies.

We wish to emphasize that the term "radio-quiet," when applied to these distant objects, generally only states that their radio luminosity is less than that of the most intense known extragalactic radio sources, and does not exclude radio emission at power levels comparable with those of typical radio galaxies. At least some of the objects previously classed as radio-quiet do show appreciable radio emission, and we conclude that the radio luminosity of blue stellar objects forms part of a continuous distribution including radio galaxies and quasistellar radio sources. There appears to be no clear-cut distinction between quasistellar radio sources and so-called quasistellar galaxies (or blue stellar objects) or between radio galaxies and normal galaxies, including the Seyfert galaxies, except in the magnitude of the phenomena that lead to radiation at radio frequencies.

VIII. SPECTRAL-INDEX DISTRIBUTION

The present observations are essentially complete for sources in the 3CR list away from the galactic plane and also include most of the identified sources north of declination −20° in the Parkes catalogues, so that a statistical study of these sources is possible. The distribution of the spectral indices between 11 and 6 cm is shown in Fig. 3 for radio galaxies, quasistellar sources, and unidentified sources. In each case, sources taken from the 3C and revised 3C catalogues are shown in black. Table IV gives the median spectral index $\bar{\alpha}$ and the dispersion σ for each group of sources between 11 and 6 cm, and also these quantities for the range 21–11 cm taken from Paper I. [The median spectral index $\bar{\alpha}$ is quoted as in Paper I, since it is less sensitive to a few extreme values. The dispersion σ is defined as half the range of α within which $\frac{2}{3}$ of the sources lie and the error in $\bar{\alpha}$ as $\sigma/(n)^{\frac{1}{2}}$, where n is the number of sources.]

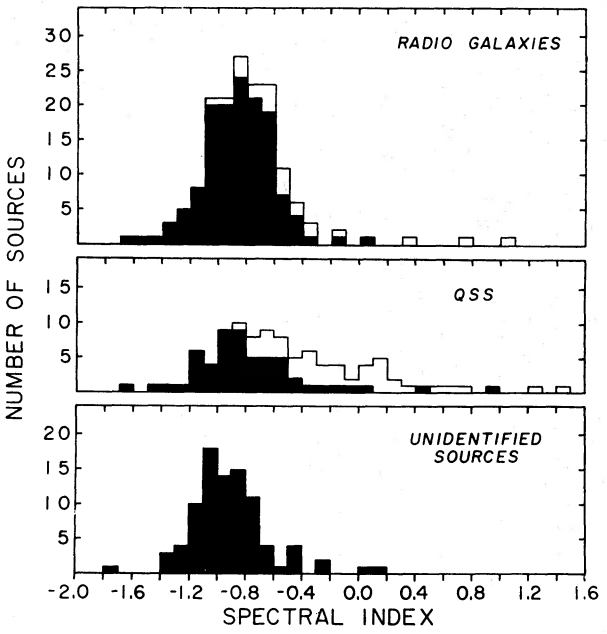

FIG. 3. Histograms of the distribution of spectral indices in the range 6–11 cm for radio galaxies (top), quasistellar sources (middle), and unidentified 3C sources at high galactic latitudes (bottom). Blackening denotes sources from the 3C catalogue.

Both the median index and dispersion for 160 radio galaxies are close to the values found between 21 and 11 cm. Inspection of the individual spectra of the radio galaxies shows that generally the spectral index is constant over the whole range from 6–21 cm. There is

TABLE IV. Median spectral index and dispersion for radio galaxies, quasistellar sources, and unidentified objects in the range 11–6 cm (present paper) and 21–11 cm (Paper I).

Class	Range 11–6 cm		Range 21–11 cm	
	$\bar{\alpha}$	σ	$\bar{\alpha}$	σ
GAL	−0.83±0.02	0.23	−0.85±0.02	0.19
QSS all	−0.59±0.05	0.46	−0.74±0.05	0.47
3C	−0.84±0.04	0.30	−0.83±0.04	0.28
PKS	−0.45±0.05	0.55	−0.60±0.07	0.50
UNID. 3C	−0.94±0.02	0.21	−0.93±0.02	0.26*

* The value of 0.33 quoted in Paper I is incorrect.

no marked difference between the spectral index distributions of the various galaxy types E, D, db, or S. The N and Seyfert galaxies, however, include a larger proportion of objects with flat radio spectra than the other types. Of the six galaxies with spectral indices more positive than −0.2, two (3C120 and 3C84) are radio-variable Seyfert galaxies, two (3C371 and Parkes 2300–18) are classified as N galaxies, the first being a radio variable, one (Parkes 1514–24) is classified as an E galaxy, and the classification of one (Parkes 0048–09) is uncertain. Thus radio galaxies are characterized by a constant spectral index from 21–6 cm, a narrow dispersion σ, and a small proportion of objects with flat spectra: the latter are mainly of the Seyfert or N type, both of which contain bright, compact nuclei.

The median index for 97 quasistellar sources (QSS) between 6 and 11 cm is significantly more positive than between 21 and 11 cm. When objects in the 3C and Parkes catalogue are considered separately, it is found that the latter have much flatter spectra and a higher dispersion than the former. Table IV shows that this difference is even more marked than in the range 21–11 cm and that this is entirely due to the median index of the Parkes QSS becoming more positive at the shorter wavelengths. The spectra of the 3C QSS resemble those of radio galaxies both in the value of the median index and in its constancy over the range 21–6 cm. The difference between the two groups of quasistellar sources is due to the difference in the frequencies at which the 3C and Parkes surveys were made. Surveys at centimeter wavelengths (Blum and Davis 1968; Kellermann, Pauliny-Toth, and Davis 1968) show that the proportion of sources with flat spectra, which is a few percent for the 3C survey, becomes larger at shorter wavelengths. The majority of sources with such flat spectra are presumably QSS of the Parkes type. They contain components of small angular size that are optically thick at centimeter wavelengths and are often variable. The luminosities of these QSS are of the order of 10^{45} ergs/sec and their linear dimensions are typically smaller than 100 pc. The 3C quasistellar sources have properties similar to those of radio galaxies: spectral indices near −0.8, absolute luminosities of 10^{42} to 10^{44} ergs/sec, and linear dimensions of tens of kiloparsecs.

In the case of unidentified sources, the present observations are only complete for the 3CR objects, since observations of unidentified sources from the Parkes catalogue tended to favor objects with flat spectra. The median index for 89 unidentified 3C sources in the range 6–11 cm is close to the index in the range 11–21 cm and corresponds to steeper a spectrum than median index of either the quasistellar sources or the radio galaxies. For radio galaxies, the slope is also constant over the whole range 6–21 cm. Bolton (1966) has suggested that the unidentified sources are very distant radio galaxies, beyond the limit of the Palomar sky survey plates and that their steep spectra between 21 and 11 cm are due to the redshift of a supposedly steeper part of the spectrum of the radio galaxies into this range. We find, however, that the spectra of radio galaxies are no steeper between 6 and 11 cm than between 11 and 21 cm, so that the steep spectra of unidentified sources in the latter range cannot be explained as the effect of a redshift. It is likely that the unidentified sources are radio galaxies rather than quasistellar sources, but the steepness of their spectra is probably due to the correlation between steep spectra and high radio luminosity (Kellermann, Pauliny-Toth, and Williams 1968). This correlation implies that in any survey of radio sources, the sources with a high luminosity and hence with steep spectra will tend to be more distant and less likely to be identified than the less luminous objects. The smaller angular size found for the unidentified sources in Sec. V(vii) is also consistent with their being distant radio galaxies.

ACKNOWLEDGMENTS

We would like to thank the operators of the 140-ft telescope for their patient and careful work, and W. E. Howard III for his helpful comments on the manuscript.

REFERENCES

Baars, J. W. M. 1966, **212**, 494.
Bennett, A. S. 1962, *Mem. Roy. Astron. Soc.* **68**, 163.
Blum, E. J. and Davis, M. M. 1968, *Astrophys. Letters* **2**, 41.
Bolton, J. G. 1966, *Nature* **211**, 1966.
Bolton, J. G., Gardner, F. F., and Mackey, M. B. 1964, *Australian J. Phys.* **17**, 340.
Braccesi, A. 1967, *Nuovo Cimento* **49**, Series X, 151.
Davis, M. M. 1967, *Bull. Astron. Inst. Neth.* **19**, 201.
Day, G. A., Shimmins, A. J., Ekers, R. D., and Cole, D. J. 1966, *Australian J. Phys.* **19**, 35.
De Jong, M. L. 1967, *Astrophys. J.* **150**, 1.
Edge, D. O., Shakeshaft, J. R., McAdam, W. B., Baldwin, J. E., and Archer, S. 1959, *Mem. Roy. Astron. Soc.* **68**, 37.
Fomalont, E. B. 1968, *Astrophys. J. Suppl.* **15**, 203.
Gower, J. F. R., Scott, P. F., and Wills, D. 1967, *Mem. Roy. Astron. Soc.* **71**, 49.
Harris, D. E., and Roberts, J. A. 1960, *Publ. Astron. Soc. Pacific* **72**, 237.
Heeschen, D. S., and Wade, C. M. 1964, *Astron. J.* **69**, 277.
Kellermann, K. I. 1966, *Australian J. Phys.* **19**, 577.
Kellermann, K. I., and Pauliny-Toth, I. I. K. 1966, *Nature* **212**, 781.
——. 1968a, *Astrophys. J.* **152**, 639.
——. 1968b, *Annual Review of Astronomy and Astrophysics* (Annual Reviews, Inc., Palo Alto, Calif.), Vol. 6, pp. 528.
Kellermann, K. I., and Pauliny-Toth, I. I. K. 1968c (to be published).
Kellermann, K. I., Pauliny-Toth, I. I. K., and Davis, M. M. 1968, *Astrophys. Letters* **2**, 105.
Kellermann, K. I., Pauliny-Toth, I. I. K., and Tyler, W. C. 1968, *Astron. J.* **73**, 298.
Kellermann, K. I., Pauliny-Toth, I. I. K., and Williams, P. J. S. 1968, *Astrophys. J.* (to be published).
Kellermann, K. I., and Read, R. B. 1965, *Publ. Owens Valley Radio Obs.* **1**, No. 2.
Kraus, J. D. 1964, *Nature* **200**, 269.
Kuril'chik, V. N., and Kokin, Yu. F. 1967, *Sov. Astron.—AJ* **11**, 374 [*Astron. Zh.* **44**, 471 (1967)].
Long, R. J., Haseler, J. B., and Elsmore, B. 1963, *Monthly Notices Roy. Astron. Soc.* **125**, 313.
MacDonald, G. H., Kenderdine, S., and Neville, A. C. 1968, *ibid.* **138**, 259.
MacDonald, G. H., Neville, A. C., and Ryle, M. 1966, *Nature* **211**, 1241.

Matthews, T. A., Morgan, W. W., and Schmidt, M. 1964, *Astrophys. J.* **140**, 35.
Medd, W. J., Locke, J. L., and Andrew, B. H. 1968, *Astron. J.* **73**, 293.
Oke, J. B., Sargent, W. L. W., Neugebauer, G., and Becklin, E. E. 1967, *Astrophys. J. Letters* **150**, L173.
Pauliny-Toth, I. I. K., and Kellermann, K. I. 1966, *Astrophys. J.* **146**, 643.
Pauliny-Toth, I. I. K., and Kellermann, K. I. 1968, *Astrophys. J. Letters* **152**, L169.
Pauliny-Toth, I. I. K., Wade, C. M., and Heeschen, D. S. 1966, *Astrophys. J. Suppl.* **13**, 65.
Pilkington, J. D. H., and Scott, P. F. 1965, *Mem. Roy. Astron. Soc.* **69**, 183.
Sandage, A. R. and Luyten, W. J. 1967, *Astrophys. J.* **148**, 767.
Shimmins, A. J., Day, G. A., Ekers, R. D., and Cole, D. J. 1966, *Australian J. Phys.* **19**, 837.
Shimmins, A. J., Searle, L., Andrew, B. H., and Brandie, G. W. 1968, *Astrophys. Letters* **1**, 167.
Zwicky, F. 1966, *Astrophys. J.* **143**, 192.

THE ASTRONOMICAL JOURNAL VOLUME 73, NUMBER 10, PART 1 DECEMBER 1968

Observations of the Phase Effect of Venus at 8.6-mm Wavelength

P. M. KALAGHAN, K. N. WULFSBERG, AND L. E. TELFORD
Air Force Cambridge Research Laboratories, Bedford, Mass.

(Received 6 August 1968; revised 25 September 1968)

Observations of the 8.6-mm brightness temperature of the planet Venus for a 12-month period centered about the inferior conjunction of 1967 have indicated a phase dependence of the form

$$T_B = 425 + 10\cos(i - 13°)\ °\mathrm{K}$$
$$(\pm 2)\quad (\pm 4)\quad (\pm 11°),$$

where the statistical standard errors are given in the lower brackets and the upper limit to all other unincluded errors is 7%. The phase-dependent term obtained is much smaller than those previously reported at this wavelength.

I. INTRODUCTION

THE purpose of this note is to describe a series of radiometric observations of the 8.6-mm brightness temperature variation of the planet Venus over the period from July 1967 to July 1968. The inferior conjunction of the planet occurred in August 1967, approximately midway in the observing period covered by the above observations and those previously reported (Kalaghan and Wulfsberg 1968).

The measurements were carried out at the Prospect Hill Radio Observatory (Waltham, Mass.), employing the AFCRL 29-ft Millimeter Wave Antenna in conjunction with a Dicke-type 8.6-mm radiometric receiving system switching between two antenna beams separated in the east–west by 15 min of arc. The half-power width of each beam, determined from measurements using a test transmitter located 10 miles away, was 4.9 $\pm$0.1 min. of arc. The antenna gain was measured to be 66.4$\pm$0.2 dB and the rms noise fluctuations of the receiver was 0.3°K for a 12-sec integration time. The particular method of observation was identical to that described previously (Kalaghan and Wulfsberg 1967).

Throughout the observational period, the brightness of the planet Jupiter was repeatedly measured in order to guard against contamination of the Venus data by undiscovered gain or pointing anomalies. Jupiter was observed on an average of two times per week for an interval of one to two hours. Venus was observed for four hours each day during the time of conjunction and for at least one hour per day for the remainder of the observational interval. The calibration noise tube was measured every 36 min of each observational period. Using the quoted gain figure, the measured brightness of Jupiter was 142°K with a statistical standard error of $\pm$6°K. This fluctuation of $\pm$6°K indicated no significant antenna gain or pointing variations in excess of $\pm$0.2 dB throughout the measurement program. The total of all other errors was estimated to be less than $\pm$7%.

Effects of stray solar radiation entering the side lobes during the time of inferior conjunction, when the sun was approximately 8° from Venus, were investigated by interspersing periods of planet tracking with periods of tracking with the antenna beams shifted slightly off the planet. No statistically significant signal level was measured during these latter "off-the-planet" trackings. We thus conclude that no data biasing occurred due to the proximity of Venus to the sun.

Atmospheric attenuation was obtained from the empirical relations of Wulfsberg (1967) using ground-level values of temperature and relative humidity recorded every hour during the observations. In approximately 10% of the observations, pointing correction factors, assuming Venus to be a uniformly bright disk, were introduced afterwards, based on boresighting observations of Jupiter and the sun. These correction factors ranged from 1.02–1.06 and averaged 1.03. The antenna temperatures were also corrected for the commensurability of the solid angle subtended